Bioorganic & Medicinal Chemistry 16 (2008) 6789–6798

Contents lists available at ScienceDirect

Bioorganic & Medicinal Chemistry

journal homepage: www.elsevier.com/locate/bmc

Conjugates of gonadotropin releasing hormone (GnRH) with carminic acid: Synthesis, generation of reactive oxygen species (ROS) and biological evaluation

Vered Lev-Goldman [a], Brenda Mester [a], Nurit Ben-Aroya [b], Tamar Hanoch [c], Barbara Rupp [d], Tsvetanka Stanoeva [d], Georg Gescheidt [d], Rony Seger [c], Yitzhak Koch [b], Lev Weiner [e,*], Mati Fridkin [a,*]

[a] Department of Organic Chemistry, The Weizmann Institute of Science, Rehovot 76100, Israel
[b] Department of Neurobiology, The Weizmann Institute of Science, Rehovot 76100, Israel
[c] Department of Biological Regulation, The Weizmann Institute of Science, Rehovot 76100, Israel
[d] Institute of Physical and Theoretical Chemistry, Graz University of Technology, Technikerstrasse 4/I, A-8010 Graz, Austria
[e] Chemical Research Support, The Weizmann Institute of Science, Rehovot 76100, Israel

ARTICLE INFO

Article history:
Received 12 March 2008
Revised 15 May 2008
Accepted 28 May 2008
Available online 19 June 2008

Keywords:
Carminic acid
Drug targeting
Reactive oxygen species (ROS)
Photosensitizer
Anthraquinone
GnRH

ABSTRACT

We synthesized two carminic acid (7-α-D-glucopyranosyl-9,10-dihydro-3,5,6,8-tetrahydroxy-1-methyl-9,10-dioxo-2-anthracene carboxlic acid, CA)-GnRH conjugates to be used as a model for potential photoactive targeted compounds. CA was conjugated to the ε-amino group of [D-Lys^6]GnRH through its carboxylic moiety or via a β-alanine spacer (β-ala). Redox potentials of CA and its conjugates were determined. We used electron spin resonance (ESR) and spin trapping techniques to study the light-stimulated redox properties of CA and its CA-GnRH conjugates. Upon irradiation, the compounds stimulated the formation of reactive oxygen species (ROS), that is, singlet oxygen ($^1O_2$) and oxygen radicals ($O_2^{-\cdot}$ and $OH^{\cdot}$). Both conjugates exhibited higher ROS production than the non-conjugated CA. The bioactivity properties of the CA conjugates and the parent peptide, [D-Lys^6]GnRH, were tested on primary rat pituitary cells. We found that the conjugates preserved the bioactivity of GnRH as illustrated by their capability to induce ERK phosphorylation and LH release.

1. Introduction

Hydroxylated 9,10-anthraquinones are natural compounds which display marked pharmacological activities and are used as anticancer and antimicrobial drugs. Among them are the anthracycline antibiotics such as daunorubicin, doxorubicin and mitomycine which form one of the largest classes of antitumor agents approved for clinical use in the cancer therapy.[1,2] The efficacy of these compounds in inhibiting cancer cell growth is believed to stem from their (a) ability to associate and intercalate with DNA duplexes and thus impair appropriate template function and nucleic acid synthesis[3]; and (b) participation in key cellular redox processes with consequent generation of highly potent reactive oxygen species (ROS), which in turn modify and degrade nucleic acids and proteins within cancer cells.[4–6] In addition to their redox activity, hydroxylated anthraquinones are also known to participate in photodynamic therapy (PDT) as photosensitizers (PSs).[7,8] PDT is a relatively new cancer treatment that involves the combination of light with a PS. While each of these factors by itself is harmless, upon irradiation in the presence of molecular oxygen they produce lethal ROS that can kill tumor cells.

Carminic acid (CA, 7-α-D-glucopyranosyl-9,10-dihydro-3,5,6,8-tetrahydroxy-1-methyl-9,10-dioxo-2-anthracene carboxlic acid) (Scheme 1) is a natural hydroxyanthraquinone derived from cochineal insect (Homoptera) grown on cacti. CA consists a sugar moiety attached to an anthraquinone. It is often used in industry as a textile dye or food colorant. As a therapeutic agent, carminic acid exhibits antiviral and antitumor activities.[9] Its interaction with biologically important redox couples, for example, iron(III, II) and copper(II, I) ions (having standard redox potentials of 0.771 and 0.153 V, respectively) was extensively studied. These interactions, especially the one involving iron, give rise to charge-transfer bands of high intensity in the visible region of absorption spectra, which are prerequisite for redox reactions, generating the free radicals.[10] In the reduced hydroquinone form, CA has been demonstrated to cause DNA nicks. Reoxidation of the CA in the hydroquinone state generates ROS such as $O_2^{-\cdot}$, H_2O_2 and $OH^{\cdot}$ radicals.[11]

In view of the non-specific toxicity of most chemotherapeutic agents toward normal cells, the development of targeted chemotherapy is highly desired. Thus, efficient targeting of chemotherapeutic drugs to inflicted areas could be of great benefit for patients with advanced or metastatic tumors. A new approach that is being developed to achieve this aim is drug targeting, first

* Corresponding authors. Tel.: +972 8 9343410; fax: +972 89 346017 (L.W.); tel.: +972 8 9342505; fax: +972 8 9344142 (M.F.).
E-mail addresses: lev.weiner@weizmann.ac.il (L. Weiner), mati.fridkin@weizmann.ac.il (M. Fridkin).

0968-0896/$ - see front matter © 2008 Elsevier Ltd. All rights reserved.
doi:10.1016/j.bmc.2008.05.057

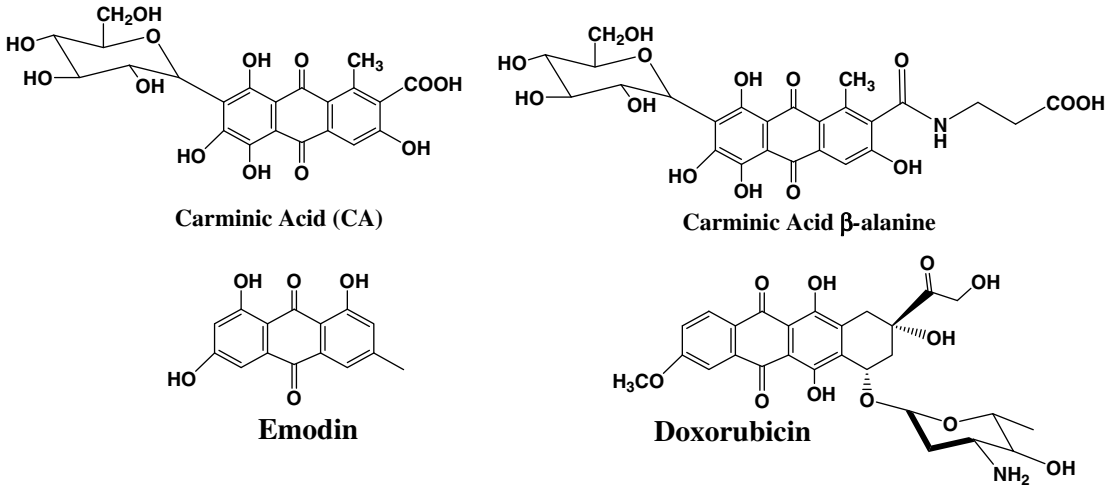

Scheme 1. Polyhydroxy-9,10-anthraquinones.

suggested by Paul Ehrlich one hundred years ago, creating the concept of a 'magic bullet'.[12,13] A vast array of methods, which can further be classified into two key approaches— active and passive have been explored for targeting drugs by means of designing innovative nanosystems.[14] Some of the methods can directly kill tumor cells or activate prodrugs specifically within the tumor (e.g., antibody-directed enzyme prodrug therapy, ADEPT). Macromolecules such as monoclonal antibodies, proteins, or peptide hormones for which specific receptors are located on cancerous cells, have been widely used as carriers for conjugation to suitable radioisotopes, drugs, or toxins.[15–19] In view of the abundance of tumors overexpressing gonadotropin hormone-releasing hormone (GnRH) receptors,[20–24] targeted chemotherapy with [D-Lys^6]GnRH employed as a vector has recently gained considerable attention.[25–28] However, because healthy pituitary gonadotropes also express GnRH receptors, [D-Lys^6]GnRH-associated drug may reach and damage these cells.[29] Such undesirable side effects can potentially be reduced or even overcome by the use of targeted photodynamic therapy (PDT), that is, through generation of ROS at desired irradiated loci.

Aiming to produce a model for an effective targeted PDT against cancer cells, we synthesized emodin (1,3,8-trihydroxy-6-methyl-9,10-anthraquinone, Scheme 1) derivatives and their GnRH conjugates. These conjugates were found to produce ROS upon illumination and preserved the affinity of the parent peptide toward its receptor. While emodin derivatives produced high levels of ROS, most of their conjugates exhibited a reduction (at different levels) in ROS levels.[30] Moreover, in a previous study, emodic acid elicited significant phototoxicity toward αT3-1 pituitary cells at a concentration of 10 μM, whereas its conjugate, [D-Lys^6(Emo)]GnRH, exhibited poor ROS production and no cell toxicity.[31,32]

The above consideration motivated us to conjugate CA to [D-Lys^6]GnRH, a potent agonist and stable form of GnRH, to assess whether the CA-peptide conjugate preserve the capacity of its components, that is, to bound to and to activate the GnRH receptor and to produce ROS that may damage cancer cells upon illumination. In this paper, we report the synthesis, redox properties, ROS photogeneration and bioactivity of CA and its GnRH conjugates.

2. Results

2.1. Synthesis

CA was conjugated through its carboxylic moiety to [D-Lys^6]GnRH (Scheme 2). For this synthesis, we first attempted direct coupling of unmodified CA using different reagents benzotriazole-1-yl-oxy-tris-pyrrolino-phosphonium hexafluoro-phosphate (PyBOP), *N*-hydroxy succininmide (NHS) and *N*,*N*′-dicyclohexylcarbodiimide (DCC), triphosgen, *N*-(3-dimethylaminopropyl)-*N*′-ethylcarbodiimide hydrochloride (EDC-HCl), 1-hydroxybenzotriazole (HOBT), and 1-[bis(dimethylamino)methylene]-1H-1,2,3-triazolo-[4,5-*b*]pyridinium hexafluorophosphate 3-oxide (HATU)—but with no success. The [D-Lys^6(CA)]GnRH conjugate was successfully synthesized only after acetylation of the hydroxyl moieties of CA followed by activating the carboxylic acid using NHS and DCC. The activated product was isolated (CA-NHS, **3**) and analyzed by MS and was further reacted with [D-Lys^6]GnRH to form the direct conjugated product (product 6). The resultant crude product was composed of a mixture of partially deacetylated products as confirmed by MS (see exp. part). We assumed that this deacetylation was due to the amino group of the [D-Lys^6]GnRH, since the peak of acetylated-[D-Lys^6]GnRH was also observed in the MS. Further deacetylation by ammonia gas was carried out to obtain the desired peptide conjugate (product 6). However, this final step hampered the synthesis causing relatively low yield (7%) and a variety of side products. Thus, β-alanine ethyl ester (β-ala) was conjugated to the acetylated CA-NHS to form product 4. After hydrolysis of the ethyl ester and the acetyl protection in one step, the purified compound was conjugated to the carrier peptide using PyBOP with 43% yield (Scheme 2).

2.2. UV–visible spectra

Figure 1 presents the UV–visible spectra of CA and its conjugates in two solvents (DMSO and PBS). CA and [D-Lys^6(β-ala-CA)]GnRH had a red shift in their λ_{max} in PBS (Fig. 1B) versus DMSO (Fig. 1A) ($\Delta\lambda_{max}$ = 32 nm). Figure 1A shows the comparison of UV–visible spectra of CA and its conjugates in DMSO. CA and its [D-Lys^6(β-ala-CA)]GnRH had the same λ_{max}, while λ_{max} of [D-Lys^6(CA)]GnRH had a red shift ($\Delta\lambda_{max}$ = 20 nm).

2.3. Redox potential

In Figure 2, the cyclovoltammogram of CA is displayed. The peak E_{pa}(−0.81 V vs SCE) indicates the first electron transfer from the electrode to the substrate led to the formation of the radical anion (anodic peak). The second (weak) peak at −1.4 V versus SCE (E_2) points to the formation of the corresponding dianion. The peaks recorded in the cathodic region indicate the partial re-oxidation of CA (E_4, −0.73 V versus SCE) together with the formation of follow-up products (E_3, E_5). These values for the reduction of CA are

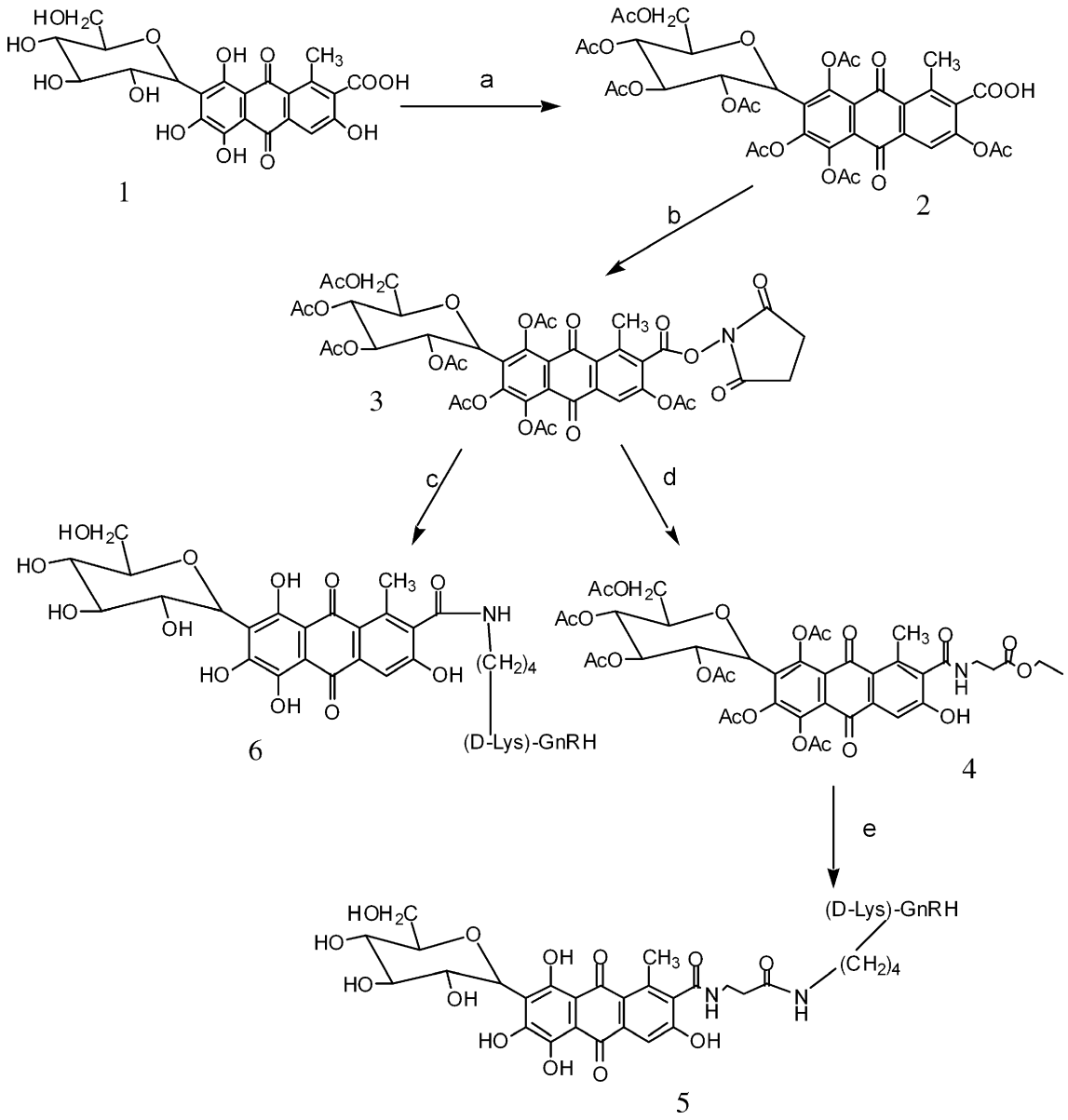

Scheme 2. Synthesis of CA-GnRH conjugates. (a) Ac_2O, Pyridine, 100 °C. (b) NHS, DCC, DMF, rt overnight. (c) 1—[D-Lys^6]GnRH, DIEPA, Dimethyl amino pyridine, DMF, rt overnight; 2—NH_3 (g), methanol, overnight. (d) β-alanine ethyl ester, DIEPA, Dimethyl amino pyridine, DMF, rt overnight. (e) 1—NaOH (1 N) in ethanol for 5 h, ice-water bath; 2—[D-Lys^6]GnRH, 4-methylmorpholine (NMM), PyBOP, DMF, rt overnight.

in good agreement with published values ($E_{1/2} = -0.736$ V versus SCE (11); with $(E_{pa} + E_4)/2 = -0.77$ V being an approximation for $E_{1/2}$).

2.4. ESR studies

CA was reduced by electrolysis. A very narrow, partially resolved ESR signal could be recorded. It is not symmetrical, being composed of two spectra (Fig. 3). The dominating pattern points to a 'doublet of doublets' associated with two non-equivalent protons. This is in agreement with a radical anion $CA^{\cdot -}$. Here, the proton at C(4) ($a_H = 0.036$ mT) and the β-proton of the sugar moiety at C(7) ($a_{H\beta} = 0.068$ mT) give rise to detectable ESR splitting, with the hyperfine coupling constants, a, of the remaining protons being very low, thus only contributing to the EPR line width (Fig. 4). Reduction of CA, CA-β-alanine, and [D-Lys^6(β-ala-CA)]GnRH with Zn in DMF unfortunately led only to weak and unresolved ESR spectra (Fig. 3). However, their width is compatible with those obtained upon electrolysis (under the assumption of a slightly higher line width, Figure 3; g factor 2.0033 throughout). Accordingly, we assume that $CA^{\cdot -}$, $[CA\text{-}\beta\text{-alanine}]^{\cdot -}$, and $[[D\text{-}Lys^6(\beta\text{-ala-CA})]GnRH]^{\cdot -}$ possess rather similar electron distributions.

Furthermore, the reduction process of CA and CA-β-alanine was followed by UV–vis spectroscopy. The spectra of the parent compounds CA and CA-β-alanine are very much alike, with an intense band at ca. 300 nm and a weaker, broad transition between 500 and 630 nm (solvent, DMSO/DMF 1:1). Compatible spectra were reported for CA in aqueous solution.[33] Upon reduction, broad bands centered at 540 (CA) and 480 (CA-β-alanine) nm emerge (Fig. 5).

2.4.1. ESR studies upon illumination

The phototoxicity of the PSs occurs most likely through two major reaction pathways: type I, involving radical cascade, electron transfer and type II, involving energy transfer, singlet oxygen production[34] (reactions 1–8). Quinones are known to participate in

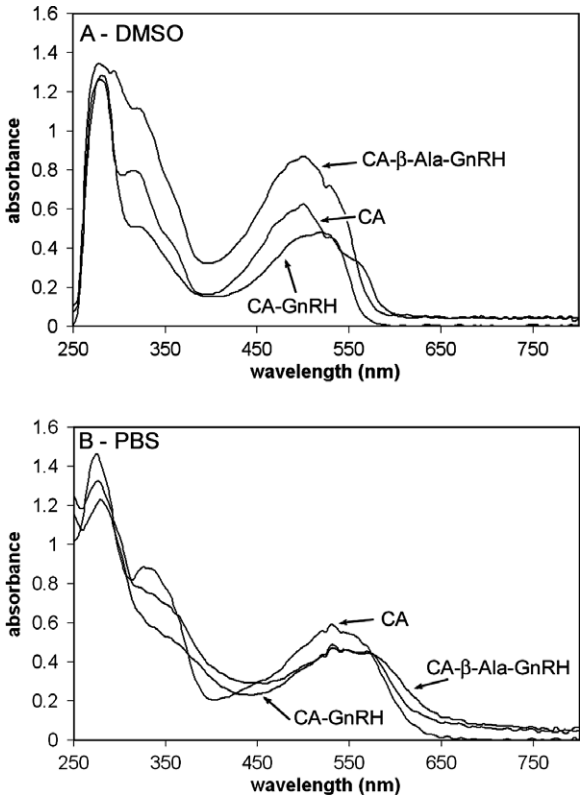

Figure 1. UV/vis spectra of 0.1 mM CA and its conjugates in (A) dimethyl sulfoxide (DMSO); (B) phosphate buffer saline (PBS, pH 7.4).

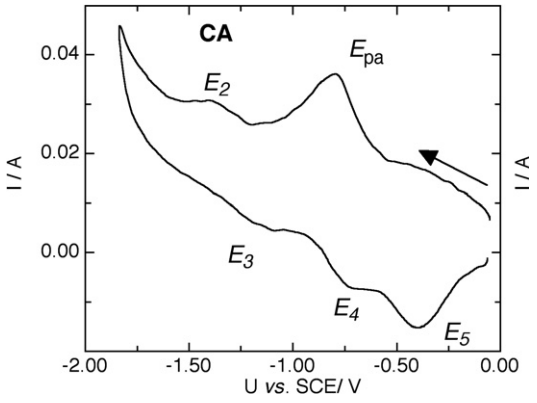

Figure 2. Cyclovoltammograms of CA (the arrow indicates the direction of the scan; scan rate: 100 mV/s).

both type I (reactions 3–6) and type II (reaction 2) photochemical reactions.[35–38]

$$Q \xrightarrow{h\nu} Q^{*} \quad (1)$$

$$Q^{*} + O_2 \rightarrow Q + {}^1O_2 \quad (2)$$

$$Q^{*} + D \rightarrow Q^{-\cdot} + D^{+\cdot} \quad (3)$$

$$Q^{-\cdot} + O_2 \leftrightarrow O_2^{-\cdot} + Q \quad (4)$$

$$O_2^{-\cdot} + O_2^{-\cdot} \xrightarrow{2H^{+}} H_2O_2 + O_2 \quad (5)$$

$$O_2^{-\cdot} + H_2O_2 \xrightarrow{Fe(cat.)} O_2 + HO^{\cdot} + OH^{-} \quad (6)$$

$$H_2O_2 + Fe(II) \rightarrow HO^{\cdot} + OH^{-} + Fe(III) \quad (7)$$

$$Q^{-\cdot} + Fe(III) \rightarrow Q + Fe(II) \quad (8)$$

Q^{*} represents quinone in an excited state;
D is electron donor; and $Q^{-\cdot}$ is semiquinone.

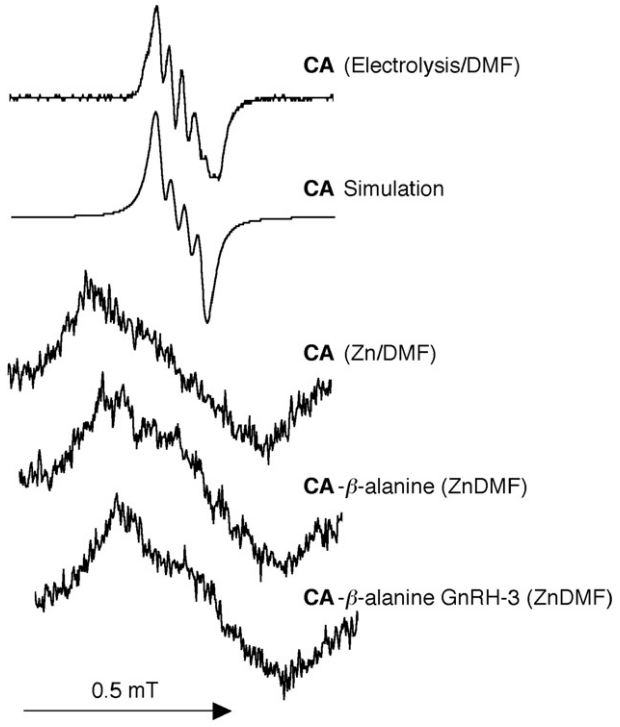

Figure 3. EPR spectrum obtained upon reduction of CA and CA-GnRH conjugate and the corresponding simulation.

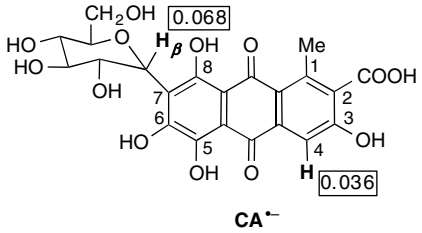

Figure 4. Assignment of *a* values in $CA^{\cdot -}$ (coupling constants are given in mT).

2.4.2. Singlet oxygen ($^1O_2$) photogeneration (type II)

Since the efficiency of anthraquinones in the inhibition of cancer cell growth is believed to be related, among other factors, to their ROS production capacity, we studied this capacity for CA and its conjugates. For testing singlet oxygen, $^1O_2$, we used the spin trap TEMP, which produces stable nitroxyl radical, TEMPO, having a triplet ESR signal (a_N = 14.8–15 G) as a result of chemical reaction with a singlet oxygen.[39] The kinetics of singlet oxygen formation was evaluated by measuring the initial rate of ESR intensity signal of the central component of the TEMPO triplet.

As shown in Figure 6, both CA and its conjugates generate singlet oxygen. In order to study the influence of the peptide carrier on singlet oxygen production, the kinetics of TEMPO adduct formation of CA, [D-Lys^6(CA)]GnRH and [D-Lys^6(β-ala-CA)]GnRH, were compared. We found that conjugation of CA with [D-Lys^6]GnRH peptide carrier increased the rate and efficacy of TEMPO formation. Notably, previous studies reported that conjugation of emodin derivatives to [D-Lys^6]GnRH decreased the level of ROS production.[30]

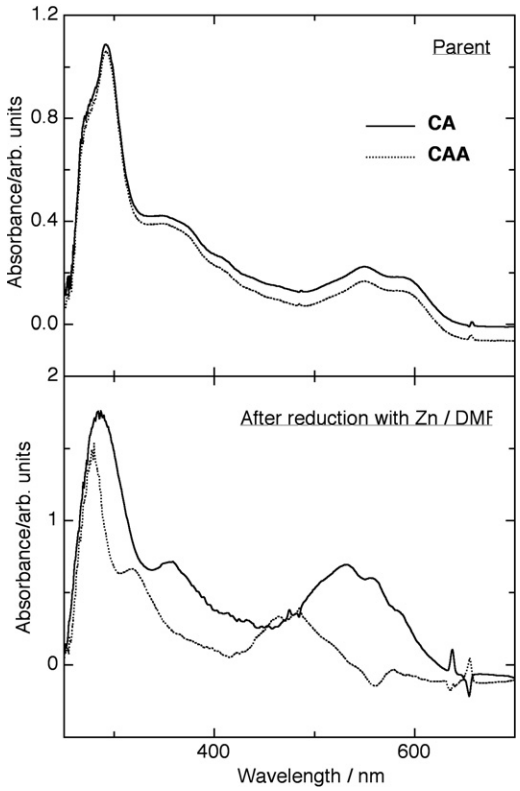

Figure 5. UV–vis spectra taken before and after reduction of carminic acid (CA) and CA-β-alanine (CAA) with Zn in DMF.

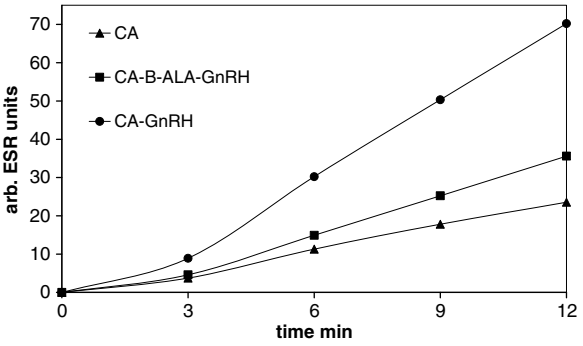

Figure 6. Effect of light on generation of TEMPO ESR signal in the presence of CA and its conjugates with white light: CA (▲), [D-Lys^6(CA-β-ala)]GnRH (■) and [D-Lys^6(CA)]GnRH (●). ESR conditions: Microwave power 31 mW, TC 1.25S, MA 1.1 G; temp. 25 °C (solvent-DMSO, components: TEMP (0.1 M); sample 1 mM).

2.4.3. Oxygen radicals photogeneration (type I)

Generation of oxygen radicals was detected by the spin trap DMPO, which reacts with short-lived radicals, such as O_2^{-}**.**, HO**.** and CH_3**·**, to produce long- lived spin adducts, each of which displays a characteristic ESR spectrum.[39]

Figure 7A shows direct production of hydroxyl-DMPO spin adduct upon irradiation in aqueous media (PBS) and NADH (quartet 1:2:2:1, $a_N = a_H^{\beta} = 14.9$ G). The spin trapping of O_2^{-}**·** by DMPO has been reported to occur along with certain artifacts. Specifically, it was shown that DMPO-OOH adduct could be spontaneously transformed to a spin adduct that is similar to the DMPO-OH ESR spectrum with the same characteristics hfc.[40–42] In order to assure the source of DMPO-OH adduct the above experiment was repeated in the presence of superoxide dismutase (SOD) (Fig. 7B). The enzyme superoxide dismutase (SOD) catalyzes the dismutation of superoxide radicals into oxygen and hydrogen peroxide. Therefore, adding SOD results in a decrease of superoxides in solution. No inhibition was observed when SOD was added to the solution of DMPO-CA. In independent experiment we also detect the formation of the hydroxyl radical using DMSO test.[43] In the presence of DMSO in the CA-DMPO solution the sextet spectrum, typical for DMPO-CH_3**.** spin adduct was observed (Fig. 7C: $a_N = 15$ G, $a_H = 22.2$ G). CH_3**.** radical can be produced only by reaction of hydroxyl radical with DMSO (*according to Eqs. 6 and 7, traces of transition metals are required for the production of hydroxyl radical. It is known that in PBS buffer there are traces of transition metals which are responsible for these reactions present.[44,45]

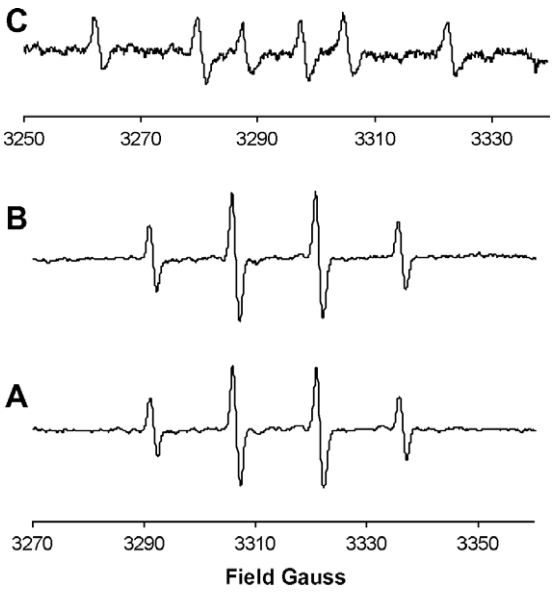

Figure 7. Effect of light (white light) on carminic acid/DMPO mixture in PBS. (A) The ESR signal represents hydroxyl-DMPO spin adduct, 4 lines, $a_N = a_H^{\beta} = 14.9$G (PBS system of 100 μL containing DMPO (0.1 M), NADH (1 mM) and Carminic acid (1 mM)). (B) The ESR signal represents hydroxyl-DMPO spin adduct as demonstrated in A and with the same intensity forming from carminic acid irradiation in the presence of superoxide dismutase (SOD). (PBS system of 100 μL containing DMPO (0.1 M), NADH (1 mM), SOD (30 μl of 1 mg/ml) and Carminic acid (1 mM)). (C) The ESR signal represents methyl-DMPO spin adduct, sixtet, $a_N = 15.6$ G, $a_H = 22.6$ G (system of PBS/DMSO, 75/15, containing NADH (1 mM), DMPO (0.1 M) and carminic acid (1 mM)).

Figure 8 shows the comparison of the intensities of the ESR signal observed for CA and its conjugates upon irradiation in 1:1

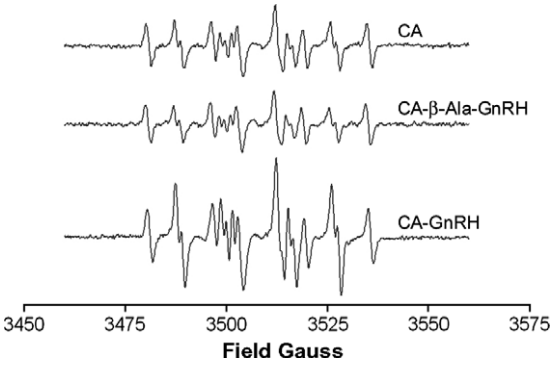

Figure 8. Effect of light on generation of DMPO-ESR signal in the presence of CA and its conjugates. The figure shows non-resolved ESR spectra composed of several types: DMPO-superoxide (12 lines, $a_N = 14.2$ G $a_H^{\beta} = 11.3$ G $a_H^{\gamma} = 1.25$ G), DMPO-CH_3 (6 lines, $a_N = 15.6$ G $a_H = 22.6$ G) and semi quinone-like signal. ESR conditions: Microwave power 31 mW, TC 1.25S, MA 1.1 G; temperature 25 °C (solvent-1:1 DMSO/PBS, components: NADH (1 mM) DMPO (0.1 M); sample 1 mM).

DMSO/PBS solvents. All ESR signals observed for CA and its conjugates in the presence of NADH were typical for superoxide-DMPO spin adduct (a_N = 14.2 G, a_H^β = 11.3 G, a_H^γ = 1.25 G) and methyl radical-DMPO spin adduct (a_N = 15 G, a_H = 22.2 G) mixture. In higher concentration of organic solvent the lifetime of superoxide anion radical is longer and reaction 5 is less effective. Moreover, a non-resolved semiquinone-like signal (g = 2.0037) was observed. However, while CA and its [D-Lys^6(β-ala-CA)]GnRH conjugate had similar intensities, [D-Lys^6(CA)]GnRH conjugate gave elevated ESR signal.

2.5. Stability of the [D-Lys^6(β-ala-CA)]GnRH conjugate toward ROS generation

ROS generated by compounds under study can react, in principle, with the peptide carriers (self damage). Stability of [D-Lys^6(β-ala-CA)]GnRH toward the ROS produced by its own irradiation is a prerequisite for specific and efficient targeting. This aspect was evaluated by HPLC analysis of the conjugate after intensive irradiation. According to the ESR measurements, ROS were efficiently formed when the mixture of [D-Lys^6(β-ala-CA)]GnRH and NADH in 1:1 PBS/DMSO was irradiated for 40 min. Analytical HPLC results showed that only as low as 5% of [D-Lys^6(β-ala-CA)]GnRH was damaged by the generated ROS, similar to other cytotoxic derivatives of [D-Lys^6]GnRH.[31]

2.6. Biological assays

2.6.1. Evaluation of LH release of [D-Lys^6(β-ala-CA)]GnRH conjugate

To evaluate the binding properties of the conjugate, bioactivity was tested. For evaluating the LH-releasing potencies of the [D-Lys^6]GnRH conjugate, rat pituitary cells were incubated in M-199 containing the desired concentrations of the tested peptide in the dark at 37 °C for 4 h, as described.[46] The bioactivity of [D-Lys^6(β-ala-CA)]GnRH and of the parent peptide [D-Lys^6]GnRH (Fig. 9) demonstrated that the agonist conjugate exhibited a similar LH releasing activity as its parent peptide, indicating that the peptide preserved its targeting ability.

2.6.2. Stimulation of ERK by [D-Lys^6(β-ala-CA)]GnRH

The extracellular signal-regulated kinase (ERK) cascade is a central pathway that transmits signals from many extracellular agents to regulate cellular processes such as proliferation, differentiation

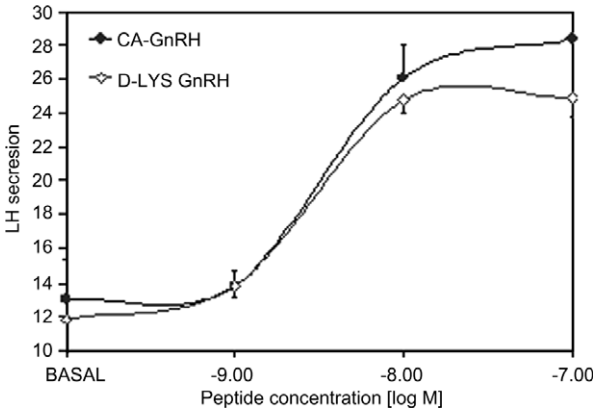

Figure 9. LH releasing potency of [D-Lys^6(β-ala-CA)]GnRH conjugate. Primary cultures of rat pituitary cells were incubated in M-199 containing the indicated concentrations of [D-Lys^6(β-ala-CA)]GnRH (•) and [D-Lys^6]GnRH (◇) for 4 h at 37 °C. The media were then collected and the LH concentration was determined by RIA. The results are means ± SEM of LH concentrations (3 wells per experimental group). The basal release after 4 h of incubation in M-199 was 13.03 ± 2.25 ng/ml.

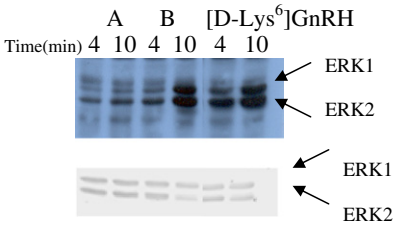

Figure 10. Stimulation of pERK1, pERK2, in αT3-1 cell line. Cells were stimulated with CA and [D-Lys^6(β-ala-CA)]GnRH (0.1 μM) for 4 and 10 min: A-CA B-[D-Lys^6(β-ala-CA)]GnRH, [D-Lys^6]GnRH as control. Each of these blots was immunoblotted with Abs to dually phosphorylated ERK (*DP*) and anti-C terminus of ERK-Ab (*C16*). The position of pERK2, ERK1, and General-ERK is indicated. Each of these experiments was reproduced at least three times.

and cell cycle progression. Signaling via the ERK cascade is mediated by sequential phosphorylation and activation of protein kinases in the different tiers of the cascade. In αT3-1 gonadotrope lineage cells, GnRH can activate ERK. GnRH rapidly increases the levels of dual phosphorylated ERKs, reaching a maximum at 5–10 min (with a gradual reduction over the subsequent 1 h).[47] Since detection of pERK is a very sensitive, it is used as readout effects of receptor-ligand stimulation.[48–50]

We measured the stimulation of phosphorylated ERK by CA relative to [D-Lys^6(β-ala-CA)]GnRH after 4 and 10 min in αT3-1 cell lines. We found that the CA conjugate stimulate ERK phosphorylation. With the [D-Lys^6]GnRH analog the stimulation increased with time from 4 to 10 min, while for CA the stimulation was less significant (Fig. 10). These results indicate that [D-Lys^6(β-ala-CA)]GnRH preserves its ability to activate ERK and which is likely modulated by binding and activation of GnRH receptor.

3. Discussion

To provide selective delivery of PS to a tumoral tissue, investigators have turned toward the targeted PS approach including conjugates containing a receptor-directing moiety and PS such as phorphyrin derivatives.[51] We selected the natural hydroxylated anthraquinone, CA, as a potentially phototoxic drug for conjugation with a peptide carrier. We presented for the first time a synthetic route by which CA was conjugated to GnRH peptide following acetylation of the hydroxyl moieties of CA. The acetylation was necessary since the structure of hydroxy-anthraquinones, that is, CA allows significant intramolecular hydrogen bonding between the hydroxyl groups, the ketones, and the carboxylic acid. Thus, in CA, the carboxylic group α to the hydroxyl group might be the reason which prevents the carboxylic group from reacting. After acetylation, we prepared octaacetyl carminic acid-*N*-hydroxysuccinimide ester, **3**, as a key intermediate, providing access to further conjugation. This was obtained either by direct conjugation with the ε-amino moiety of Lys6 in the agonist GnRH analog to form conjugate **6**, [D-Lys^6(CA)]GnRH, or by using a spacer, that is, β-alanine ethyl ester, to form conjugate **5**, [D-Lys^6(β-ala-CA)]GnRH.

As follows from reaction 3, interaction of quinone in excited state with biological electron donor generates semi-quinone (we used NADH). Semi quinone is crucial for electron transfer and creation of superoxide and hydroxyl radical as well as for reduction of Fe(III). Therefore, we applied a repertoire of physico-chemical methods for describing the semi quinone moiety. The reduction potential of CA (−0.81 V vs SCE (E_{pa}) is lower than that of anthraquinone (E_{pa} = −0.92 V vs SCE) under identical experimental conditions. The reduction potential of anthraquinone derivatives is markedly dependent on the substituents at the π system. The presence of hydroxy groups leads to reduction at less negative potentials. This can be accounted for by the electron-withdrawing

effect of the carboxylic group at C(2) and the hydroxy substituents at C(3,5,6,8). The presence of OH groups directly attached to the π system of the anthraquinone skeleton is very likely the cause for the more complex cyclovoltammogram of CA. Such complexity presumably mirrors protonated-deprotonated stages, particularly for the adjacent OH groups at C(5) and C(6) where a stable internal O···H···O bridge is feasible. Consequently, the anthraquinone moiety in CA and its derivatives is the electro-active part in these molecules.

The good agreement between the experimental and the calculated a_H values, indicates that, the spin and the charge are exclusively delocalized within the anthraquinone π system, consistent with the redox potentials. The reason for the rather narrow ESR spectra with small a_H values is that only the protons H–C(4) and H_β–C–C(7) carry a sufficient spin population to be detected in the ESR spectrum; the remaining protons being either attached to positions with low spin population or too distant to possess detectable hyperfine coupling constants (Fig. 11). The considerably lower resolution of the ESR spectrum of CA, CA-β-alanine, and [D-Lys^6(β-ala-CA)]GnRH obtained after reduction with Zn in DMF points to association phenomena between the corresponding radical anions and the Zn^{2+} cation (not unexpected in terms of the numerous hydroxy, amino, and carboxy groups present in CA, CA-β-alanine, and [D-Lys^6(β-ala-CA)]GnRH).

The close relationship between the electronic structures of CA and its derivatives is additionally illustrated by the rather similar electronic spectra of the parent molecules and the one-electron-reduced species. The coupling of the anthraquinone derivatives to a peptide carrier does not significantly affect the redox potential. On the other hand, the (bulky) peptide carrier influences the conformational dynamics of the methylene group connecting the π system with the peptide. This might cause a rather rigid arrangement of the peptide.

Previous studies on CA mixed with Fe(II,III) and Cu(II,III) were carried out by UV–visible and IR spectroscopy. These studies did not reveal superoxide radical anions (using NBT method) for most of the oxygenated metal–CA mixture solutions. On the other hand, spectral evidence for oxidative activation of CA was obtained.[10] We found that CA can produce ROS upon irradiation as shown in our ESR results (Figs. 6–8). These results prompted us to conjugate CA to [D-Lys^6]GnRH as the peptide carrier.

When irradiated, CA and its conjugates stimulated the formation of singlet oxygen, $^1O_2$, (Fig. 6) and oxygen radicals (Fig. 7, 8). However, there were differences in the ROS production efficacy by these derivatives: CA conjugates produced the strongest ESR signals of detected spin adducts compared to CA alone. Apparently, the conjugation with the peptide elevates ROS production. This view is in accord with a previous report showing that increase in ROS production may be attributed to the electronic effect of the amino acids of the peptide, for example, tryptophan and tyrosine.[52]

Most photosensitizers are hydrophobic and hence tend to aggregate in aqueous media as a result of the propensity of the hydrophobic skeleton to avoid contact with water molecules.[35,53]

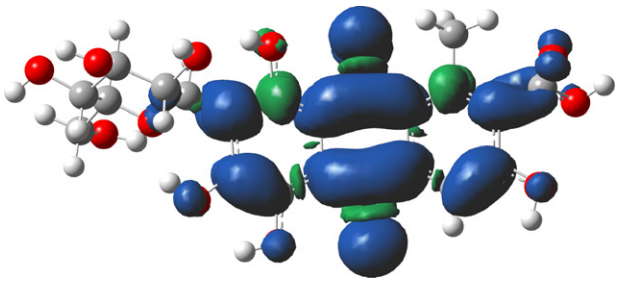

Figure 11. Spin-density distribution in $CA^{\cdot-}$.

It was suggested that the different behavior of CA and its GnRH conjugates in organic solvents versus PBS can stem from appearance of aggregates of the quinones in PBS but not in organic solvents where the skeleton of CA remains in a monomeric form. For quinone in a monomeric form, energy transfer could be more effective. This was studied for a well-known PS, hypericin.[35] Therefore, we detected typical singlet oxygen-ESR signal for CA and its GnRH conjugates when an organic solvent (DMSO) was used (Fig. 6), but we could not detect it in water medium (PBS). This reasoning was supported by red shift in UV spectrum of CA in PBS vs. DMSO; $\Delta\lambda_{max} = \Delta 32$ nm (Fig. 1A).

The direct production of DMPO-OH spin addict was assessed by irradiation of CA and DMPO in PBS buffer (Fig. 7). The production of the methyl-ESR signal by NADH in Figure. 7C can be accounted for by the production of the semiquinone by the electron donor, which in turn produced superoxide. In the presence of water media, the superoxide stimulated hydrogen peroxide (H_2O_2) and hydroxyl radical ($OH^{\cdot}$) production.[36] DMSO is known to react with a hydroxyl radical at a high rate to generate a methyl radical ($CH_3^{\cdot}$), which can be trapped by DMPO and identified by its characteristic hyperfine pattern.[43] The results presented by Figures 7(A–C) showed that CA can produce hydroxyl radical ($OH^{\cdot}$) upon irradiation. Neither superoxide nor hydrogen peroxide is particularly toxic to the cell. It is the product of their reaction, hydroxyl radical ($HO^{\cdot}$), which is thought to mediate most radical cytotoxicity.

Although [D-Lys^6(CA)]GnRH produced the strongest ESR signal, its synthesis proceeded with difficulties and low yield. This fact resulted, probably, from steric hindrance by coupling the activated ester of the CA molecule with the close acetylated groups with the peptide. Therefore, we focused on the indirect conjugate [D-Lys^6(β-ala-CA)]GnRH for the biological tests. The stability of the [D-Lys^6(β-ala-CA)]GnRH conjugate was tested under irradiation conditions and 5% degradation was found after 40 min under these conditions.

We hypothesized that the conjugation of CA to GnRH analogs may be a selective way of destroying cancer cells through direct illumination of the tumor site. Breast, prostate and other types of cancers often express GnRH receptors, and GnRH analogs have been found to exert direct antiproliferative effect on related cancer cells.[23,24] [D-Lys^6]GnRH was chosen since it can be conjugated to CA via the only free amino group in position 6. [D-Lys^6]GnRH conjugates were shown to bind with high affinity to the GnRH receptors, induce LH release from pituitary cells and be internalized by receptor mediated mechanism.[25,54] The ability of the conjugate to be internalized inside the cell is of most importance since the diffusion distances of the ROS produced upon irradiation were reported to be very short.[55] We therefore studied the bioactivity properties of [D-Lys^6(β-ala-CA)]GnRH compared to the parent peptide, [D-Lys^6]GnRH. Investigation of the in vitro LH releasing potencies, carried out in the dark, together with the pERK stimulation results, demonstrated that [D-Lys^6(β-ala-CA)]GnRH preserves its selectivity toward GnRH receptors (Figs. 10, 11). Based on previous studies[32,56] and on results presented here, it is expected that this potential phototoxic conjugate would bind specifically to cells that express GnRH receptors. Further, the redox properties, ROS photogeneration, as well as binding capacity of CA-GnRH conjugates demonstrated in this present study are prerequisite for possible and successful biological phototoxic effects.

4. Experimental

4.1. Reagents

Carminic acid (CA), 2,2,6,6-tetramethyl piperidine (TEMP), 5,5′-dimethyl-pyroline *N*-oxide (DMPO) and β-nicotinamide adenine

dinucleotide (NADH) were obtained from Sigma–Aldrich Chemical Co. (St. Louis, MO, USA). The colored impurity present in the commercial DMPO was removed by treatment with neutral decolorizing charcoal.[57]

4.2. General procedures

Nuclear magnetic resonance (NMR) spectra were recorded at 25 °C on Bruker spectrometers (250 MHz and 400 MHz, Karlsruhe, Germany). Mass spectrometry (MS) was performed on a Micromass Platform LCZ 4000 (Manchester, UK) utilizing the electron spray ionization (ESI) method. Reversed-phase high-performance liquid chromatography (HPLC) was performed on a Spectra-Physics SP-8800 liquid chromatography system equipped with an Applied Biosystems 757 variable wavelength absorbance detector at 220 nm. HPLC prepacked columns used were: VYDAC RP-18 column (250×22 mm; 10 μm, Vydac, Hesperia, CA 10 ml/min) for semi-preparative purification and Chromolith™ RP-18e column (4.6 × 100 mm; Merck, Darmstadt, Germany) for analytical purposes. HPLC purifications and analyses were achieved by using as eluent a linear gradient established between 0.1% trifluoroacetic acid (TFA) in water as solvent A and 0.1% TFA in 75% aqueous acetonitrile as solvent B. The purity of all synthetic peptides and conjugates was screened by analytical HPLC eluent varying from 10 to 100% B in 10 min, 3 ml/min. The crude synthetic CA derivatives and its conjugates were purified using binary A/B gradients. Eluent composition was 10%B for the first 10 min, increasing linearly to 100% B after 60 min, 10 ml/min. Chromatograms were recorded on a Chrom-Jey SP-4270 electronic integrator. For amino acid composition analysis, peptides were hydrolyzed in 6 N HCl at 110 °C for 22 h under vacuum, and the hydrolysates were analyzed with a Dionex Automatic Amino Acid Analyzer.

4.3. General peptide synthesis

Unless indicated otherwise, all peptides were synthesized on an automatic multiple peptide synthesizer (AMS-422, Abimed-Technik GnbH, Langenfeld, Germany) with Rink amide resin as a polymeric support following the company's protocol for Fmoc strategy as described.[58,59]

4.3.1. Octaacetyl carminic acid (2)

A solution containing carminic acid, **1** (60 mg, 0.12 mmol), acetic anhydride (1.1 ml, 11.6 mmol), and pyridine (390 μl) was heated to 100 °C. The progress of the acetylation reaction was followed by analytical HPLC indicating the disappearance of all the CA and the appearance of two new peaks, corresponding to octaacetyl carminic acid and small amounts of heptaacetyl carminic acid. For analytical purpose, a portion (1/3 from the total amount) from this mixture was purified by semi-preparative HPLC. ^{1}H NMR ($CDCl_3$, δ, 250 MHz): 1.94–2.01 (m, OAc, 12 H), 2.21–2.46 (m, OAc, 12H), 2.59(s, ar-CH_3), 3.72 (m, 5′H), 3.91 (m, 6′H^a), 4.35 (m, 6′H^b), 4.70 (d, J = 9.81 Hz, 1′H), 4.86 (d, J = 9.03 Hz, 1′H), 5.11 (m, 4′H), 5.23(m, 3′H), 5.55 (m, 2′H), 5.67 (m, 2′H), 7.75 and 7.72 (2s, ar-H). Mass spectrometry: found m/z $[M-H]^+$ = 827.4; calcd. for $C_{38}H_{35}O_{21}$ $[M-H]^+$ = 827.7; Mass spectrometry found for heptaacetyl-carminic acid m/z $[M-H]^+$ = 785.4; calcd. for $C_{36}H_{33}O_{20}$ $[M-H]^+$ = 785.6.

4.3.2. Octaacetyl carminic acid-*N*-hydroxysuccinimide ester (3)

To the reaction mixture of the crude **2** in 500 μl *N*,*N*′-dimethylformamide (DMF) were added NHS (24.75 mg, 0.21 mmol) and DCC (44.55 mg, 216 μL of 1 M solution in DMF. The solution was stirred at room temperature overnight and purified by semi-preparative HPLC. The fraction containing the desired product was lyophilized to yield a yellow powder (27 mg; yield 24%). The product contained as well a minor product with hepta- and hexa-acetyl groups as observed in the M.S. results. Mass spectrometry: found m/z $[M+Na^+]^+$ = 948.9; calcd. for $C_{42}H_{39}NO_{23}$ $[M+Na^+]^+$ = 948.7 and for hepta-product found m/z $[M+Na^+]^+$ = 906.9; calcd. for $C_{40}H_{37}NO_{22}$ $[M+Na^+]^+$ = 906.7; and for hexa-product found m/z $[M+Na^+]^+$ = 864.8; calcd. for $C_{38}H_{35}NO_{21}$ $[M+Na^+]^+$ = 864.7.

4.3.3. Tetraacetyl carminic acid-β-alanine ethylester (4)

A mixture containing product **3** (13 mg, 0.014 mmol), β-alanine ethyl ester (107 mg, 0.7 mmol), diisopropyl amine (DIEPA) (122 μl, 0.7 mmol), dimethyl amino pyridine (0.2 mg, 1.4 μmol) and 500 μl DMF was stirred overnight at room temperature. The product was purified by semi-preparative HPLC to receive 4 mg of purified product (yield 37%). ^{1}H NMR ($CDCl_3$, δ, 250 MHz): 1.23 (m, CH_3-ethyl), 1.78–2.04 (m, OAc, 12H), 2.68(br s, ar-CH_3+ CH_2CO_2–, 5H), 3.73 (m, C(O)–NH–CH_2, 2H), 3.82–5.90 (m, glucose and CO_2CH_2, 7H), 6.87 (s, NH), 7.51 (s, ar-H). Mass spectrometry: found m/z $[M-H^+]^+$ = 757.4; calcd. for $C_{35}H_{36}NO_{18}$ $[M-H]^+$ = 757.7.

4.3.4. Carminic acid-β-alanine (5)

Solution of product **4** (4 mg, 5 μmol) in sodium hydroxide (40 μL, 1 N) and ethanol (300 μL absolute) was stirred with ice-water bath for 5 h. The progress of the hydrolysis reaction was checked by analytical HPLC. Following its completion, without further purification, the reaction mixture was lyophilized to receive 2 mg product (70% yield) and analyzed by M.S. Mass spectrometry: found m/z $[M-H^+]^+$ =562.1; calcd. for $C_{25}H_{24}NO_{14}$ $[M-H]^+$ = 562.5.

4.3.5. [D-Lys^6(CA)]GnRH

Solution of product **3** (11.27 mg, 0.012 mmol), [D-Lys^6]GnRH (66.8 mg, 0.052 mmol), DIEPA (47 μl, 0.27 mmol), dimethyl amino pyridine (1.65 mg, 0.015 mmol) and 600 μl DMF was stirred over night at room temperature and the reaction was monitored by analytical HPLC. The product was fractionated by semi-preparative HPLC. Three isolated peaks were found related to the desired product, showing molecular weights corresponding to conjugates containing 2, 3, and 4 acetyl groups. The peaks were combined for the next step and lyophilized to receive total mass of 5.7 mg (25% yield). The conjugates were analyzed by MS and amino acid analysis. Mass spectrometry: found m/z: $[M1+H]^+$ = 1981.3 (-2Ac); $[M2+H]^+$ = 1939.9 (-3Ac); $[M3+H]^+$ = 1898.4 (-4Ac). calcd. for M1(-2Ac) $C_{93}H_{116}N_{18}O_{31}$ $[M+H]^+$ = 1982.1. calcd. for M2(-3Ac) $C_{91}H_{114}N_{18}O_{30}$ $[M+H]^+$ = 1940.1. calcd. for M3(-4Ac) $C_{89}H_{112}N_{18}O_{29}$ $[M+H]^+$ = 1898.1.

4.3.5.1. Amino acid analysis. His 0.68,[1.0] Ser 1,[2.0] Asp+Asn 5.31,[5.0] Ala 2.26,[2.0] Val 2.15,[2.0] Phe 1.10,[1.0] Thr 2.08,[2.0] Tyr 1.98,[2.0] Arg 2.28,[2.0] Leu 3.11,[3.0] Lys 3.21,[3.0] Gln 1.08,[1.0] Nleu 1.06,[1.0] Ile 1.05.[1.0].

Removal of the acetyl groups was done by dissolving in 15 ml methanol while ammonia gas (dried over sodium hydroxide) was bubbled for 3 h through the solution and the reaction mixture was left overnight in a closed round-bottom flask with stirring. The product was isolated by HPLC (1.56 mg, 7% total yield). It was characterized by MS and UV/visible spectra (Fig. 1). Mass spectrometry m/z $[M+H^+]$ = 1728.3; calcd m/z for $C_{80}H_{101}N_{18}O_{26}$ $[M+H^+]$ = 1730.8.

4.3.6. [D-Lys^6(β-ala-CA)]GnRH

[D-Lys^6]GnRH (5 mg, 3.9 μmol) was dissolved in DMF (300 μL). Carminic acid-β-alanine, **5** (2 mg, 3.5 μmol), 4-methylmorpholine (4-NMM, 2.5 μL), and PyBOP (1.7 mg, 3.6μL) were added. The mixture was stirred for 4 h at room temperature. The progress of the reaction was followed by the disappearance of [D-Lys^6]GnRH as revealed by analytical HPLC. Upon completion of the reaction, the crude peptide was precipitated with ice-cold *tert*-butyl methyl

ether (3 ml), collected by centrifugation and dried. The peptide was then purified by semi-preparative HPLC to give 2.86 mg (43% yield). The conjugate was analyzed by Mass spectrometry *m/z* $[M+H^+]$ = 1800.5; calcd *m/z* for $C_{84}H_{108}N_{19}O_{26}$ $[M+H^+]$ = 1799.9 and UV/visible spectra (Fig. 1).

4.4. Cyclovoltammetry

Polarecord E 506, VA scanner E 612, VA stand 633 (Methrom,, Switzerland) connected to LabView (National Instruments, USA), and Uniscan Instruments (UK) PG580 potentiostat were used for the analysis. The working electrode was Pt-Disk, counter electrode Pt wire and the reference electrode Ag wire. At the end of the measurements, ferrocene was added to the solution, and its half-wave potential was used as an internal reference. Values were recalculated to SCE (standard calomel electrode) as the standard. The supporting electrolyte was tetrabutylammonium perchlorate (0.1 M). All measurements were performed under N_2 at room temperature in acetonitrile (dried over molecular sieves and distilled).

4.5. Electron spin resonance (ESR)

Redox reactions of the parent molecules were performed by in situ electrolysis inside the ESR cavity (working electrode, Au-Helix; counter electrode, Pt wire). $T = -40$ °C. ESR spectra were taken on a Varian E9 spectrometer equipped with a Hewlett Packard 5350B Microwave Frequency Counter and an ER 0.35 M Gaussmeter (Bruker, Germany) for the determination of *g* values.

4.5.1. Photoexcitation of CA and its GnRH conjugates

Spin trapping studies were performed with a Bruker Electron Spin Resonance ELEXYS-500 spectrometer at 25 °C. All irradiations were carried out with a KL 1500 electronic projector lamp (Schott. Mainz, Germany). Samples were irradiated directly inside the ESR cavity with an optical fiber while the ESR spectra were recorded. White light and filters with λ_{max} = 527 nm were used. For spin trapping studies, a mixture of DMPO (0.1 M) or TEMP (0.1 M) and CA or its conjugates (1 mM) was irradiated in a 70 μL and 100 μL quartz ESR flat cells. Biological reducing compounds, NADPH, NADH, were used as potential donors in light stimulated ROS generation. The enzyme superoxide dismutase, (SOD), was used to assess the production of hydroxyl radical.

4.6. UV–vis spectroscopy of reduction

J&M Tidas (J&M, Aalen, Germany) fiber-optics, diode array spectrometer were adjusted for the measurement of UV-vis spectra in ESR tubes. [Solvent, DMF was dried over molecular sieves]. All samples were prepared under N_2.

4.7. Calculations

The Gaussian 98 software package[60] was used throughout. Geometry optimizations and calculations of the hyperfine coupling constants, *a*, were performed at the B3LYP/6-31G-d level of theory.

4.8. Biological assay

Effect of [D-Lys⁶(β-ala-CA)]GnRH on luteinizing hormone (LH) release. The LH-releasing potencies of the GnRH conjugate and its parent peptide were evaluated in primary pituitary cell cultures prepared from 21-day-old Wistar-derived female rats as described earlier.[46] Cultures were maintained in M-199 medium supplemented with 10% horse serum and antibiotics and were plated (50,000 cells/well) in 96-multiwell tissue culture dishes. After 48 h, the medium was replaced by phenol red and serum-free M-199 containing the desired concentration of the peptides (three wells/experimental group) was added. Plates were then incubated in the dark at 37 °C for additional 4 h. The experiments were carried out in the dark to avoid photo-activation of the CA derivative moiety. At the end of the incubation period, supernatants (0.1 mL) were diluted with 1% BSA/PBS (0.9 mL) and analyzed for LH content by double-antibody RIA[61,62] using kits kindly supplied by the National Institute of Arthritis, Metabolism and Digestive Diseases (NIMDD).

4.9. Determination of ERK activity

αT3-1 cells were serum-starved for 18 h in Dulbecco's modified Eagle's medium containing 0.1% fetal calf serum, after which the examined stimulants (CA and its conjugate, 0.1 μM) were added for 4 and 10 min, separately. After removal of medium, cells were rinsed twice with ice-cold PBS. Then, the cells were lysed with 160 μL of ice cold RIPA buffer which was added for 10 min on ice (RIPA buffer: 137 mM NaCl, 20 mM Tris, pH 7.4, 10% (v/v/) glycerol, 1% (v/v) Triton X-100, 0.5% (w/v) Deoxycholate, 0.1% (w/v) SDS, 2.0 mM EDTA, 1.0 mM phenylmethylsulphonyl fluoride (PMSF, added fresh, and 20 μM Leupeptin). The extracts were centrifuged (100,000*g*, 15 min, 4 °C), and the supernatants, containing the cytosolic and nuclear proteins, were further kept at 4 °C. The supernatants were then resolved by a 10% SDS–PAGE, transferred onto a nitrocellulose membrane, and probed with appropriate antibodies (Abs). Abs binding was detected using ECL (Amersham Pharmacia Biotech) according to the manufacturer's instructions. The Abs used were anti-general ERK and anti-DP-ERK (Sigma, Rehovot, Israel).

Acknowledgments

We thank Ms. Rubinraut Sara and Kapitkovsky Aviva for the synthesis of the GnRH Peptides. M.F. is the Lester Pearson Professor of Protein Chemistry. Y.K. is the Adlai E. Stevenson III Professor of Endocrinology and Reproductive Biology. This work was supported by a grant of the Israel Science Foundation (703939).

References and notes

1. Powis, G. *Free Radic. Biol. Med.* **1989**, *6*, 63.
2. Moore, H. W.; Czerniak, R.; Hemdan, A. *Drug Expl. Clin. Res.* **1986**, *12*, 475.
3. Crooke, S. T.; Duvernay, V. H.; Mong, S. In *Molecular Actions and Targeted for Cancer Chemotherapeutic Agents*; Sartorelli, A. C., Lazo, J. S., Bertino, J. R., Eds.; Academic Press: New York, NY, 1981; pp 137–160.
4. Pacifici, R. E.; Davies, K. J. A. *Methods Enzymol.* **1990**, *186*, 485.
5. Bukit, M. J.; Fitchett, M.; Gilbert, B. C. In *Free-Radical Damage to nucleic Acid Compounds by the Fenton Reaction: An ESR Study*; Hayaishi, O., Niki, E., Kondo, M., Yoshikawa, T., Eds.; Elsevier: Amsterdam, 1989; pp 63–70.
6. Stsdtman, E. R. *Annu. Rev. Biochem.* **1993**, *62*, 797.
7. Gollinick, K.; Held, S.; Martire, D. O.; Braslavsky, S. E. *J. Photochem. Photobiol. A: Chem.* **1992**, *69*, 155.
8. Dabestani, R.; Hall, R. D.; Sik, R. H.; Chignell, C. F. *Photochem. Photobiol.* **1990**, *52*, 961.
9. Jamison, J.; Flowers, D.; Jamison, E.; Kitareewan, S.; Krabill, K.; Rosenthal, K.; Tsari, C. *Life Sci.* **1988**, *42*, 1477.
10. Tutem, E.; Apak, R.; Sozgen, K. *J. Inorg. Chem.* **1996**, *61*, 79.
11. Lown, J. W.; Chen, H.; Sim, S.; Plambeck, A. J. *Bioorg. Chem.* **1979**, *8*, 17.
12. Erlich, P.. In *The Collected Papers of Paul Ehrlich, edc*; Himmelweite, F., Marrquardt, M., Dale, H., Eds.; Pergamon: Elmsford, NY, 1956; vol. 1, pp 596–618.
13. Schwartz, R. S. *N. Engl. J. Med.* **2004**, *350*, 1079.
14. Vasir, J. K.; Reddy, M. R.; Labhasetwar, V. D. *Curr. Nanosci.* **2005**, *1*, 47.
15. Torchilin, V. P. *Eur. J. Pharm. Sci.* **2000**, *2*, S81.
16. Bagshawe, D. K. *Drug Dev. Res.* **2004**, *34*, 220.
17. Vitetta, E. S.; Krolick, K. A.; Miyama-Inaba, M.; Cushley, W.; Uhr, J. W. *Science* **1983**, *219*, 644.
18. Schally, A. V.; Nagy, A. *Trends Endocrinol. Metab.* **2004**, *15*, 300.
19. Bagshawe, K. D.; Sharma, S. K.; Springer, C. J.; Rogers, G. T. *Ann. Oncol.* **1994**, *5*, 879.
20. Kakar, S.; Grizzle, W.; Neil, J. *Mol. Cell. Endocrinol.* **1994**, *106*, 145.
21. Eidne, K.; Flanagan, C.; Harries, N.; Millar, R. *J. Clin. Endocr. Metab.* **1987**, *64*, 425.

22. Quayam, A.; Gullick, W.; Clayton, RC.; Sikora, K.; Waxman, J. *Br. J. Cancer* **1990**, *62*, 96.
23. Chen, A.; Kaganovsky, E.; Rahimipour, S.; Ben-Aroya, N.; Okon, E.; Koch, Y. *Cancer Res.* **2002**, *62*, 1036.
24. Volker, P.; Grundker, C.; Schmidt, O.; Schulz, K. D.; Emons, G. *Am. J. Obstet. Gynecol.* **2002**, *186*, 171.
25. Hazum, E.; Meidan, R.; Liscovitch, M.; Keinan, D.; Linder, H. R.; Koch, Y. *Mol. Cell. Endocrinol.* **1983**, *30*, 291.
26. Bajusz, S.; Janaky, T.; Csemus, V. J.; Bokser, L.; Fekete, M.; Srkalovic, G.; Redding, T. W.; Schally, A. V. *Proc. Natl. Acad. Sci. U.S.A.* **1989**, *86*, 6318.
27. Janaky, T.; Juhasz, A.; Bajusz, S.; Csernus, V.; Srkalovic, G.; Bokser, L.; Milovanovic, S.; Redding, T. W.; Rekasi, Z.; Nagy, A.; Schally, A. V. *Proc. Natl. Acad. Sci. U.S.A.* **1992**, *89*, 972.
28. Nagy, A.; Schally, A. V.; Armatis, P.; Szepeshazi, K.; Halmos, G.; Kovacs, M.; Zarandi, M.; Groot, K.; Miyazaki, M.; Jungwirth, A.; Horvath, J. *Proc. Natl. Acad. Sci. U.S.A.* **1996**, *93*, 7269.
29. Kovacs, M.; Schally, A. V.; Nagy, A.; Koppan, M.; Groot, K. *Proc. Natl. Acad. Sci. U.S.A.* **1997**, *94*, 1420.
30. Lev-Goldman, V.; Mester, B.; Ben-Aroya, N.; Koch, Y.; Weiner, L.; Fridkin, M. *Bioconj. Chem.* **2006**, *17*, 1008.
31. Rahimipour, S.; Bilkis, I.; Peron, V.; Gescheidt, G.; Barbosa, F.; Mazur, Y.; Koch, Y.; Weiner, L.; Fridkin, M. *Photochem. Photobiol.* **2001**, *74*, 226.
32. Rahimipour, S.; Ben-Aroya, N.; Koch, Y.; Fridkin, M. *J. Med. Chem.* **2001**, *44*, 3645.
33. Favaro, G.; Miliani, C.; Romani, A.; Vagnini, M. *J. Chem. Soc., Perkin Trans.* **2002**, *2*, 192.
34. Foote, C. S. *Photochem. Photobiol.* **1991**, *54*, 659.
35. Weiner, L.; Roth, E.; Mazur, Y.; Silman, I. *Biochemistry* **1999**, *38*, 11401.
36. Wu, T.; Shen, J.; Song, A.; Chen, S.; Zhang, M.; Shen, T. *J. Photochem. Photobiol. B Biol.* **2000**, *57*, 14.
37. Diwu, Z.; Lown, J. W. *Photochem. Photobiol.* **1990**, *52*, 609.
38. Rahimipor, S.; Palivan, C.; Barbosa, F.; Bilkis, I.; Koch, Y.; Weiner, L.; Fridkin, M.; Mazur, Y.; Gescheidt, G. *J. Am. Chem. Soc.* **2003**, *125*, 1376.
39. Buettner, G. R. *Free Rad. Biol. Med.* **1987**, *3*, 259.
40. Finkelstein, E.; Rosen, G. M.; Rauckman, E. J. *J. Am. Chem. Soc.* **1980**, *102*, 4994.
41. Finkelstein, E.; Rosen, G. M.; Rauckman, E. J. *Mol. Pharmacol.* **1982**, *21*, 262.
42. Chignell, C. F.; Motten, A. G.; Sik, R. H.; Parker, C. E.; Reszka, K. *Photochem. Photobiol.* **1994**, *59*, 5.
43. Weiner, L. *Methods Enzymol.* **1994**, *233*, 92.
44. Sushkov, D. G.; Gritsan, N. P.; Weiner, L. M. *FEBS Lett.* **1987**, *225*, 139.
45. Kalyanaraman, B.; Morehouse, K. M.; Mason, R. P. *Arch. Biochem. Biophys.* **1991**, *286*, 164.
46. Yahalom, D.; Rahimipour, S.; Ben-Aroya, N.; Koch, Y.; Fridkin, M. *J. Med. Chem.* **2000**, *43*, 2824.
47. Yoon, S.; Seger, R. *Growth Factors* **2006**, *24*, 21.
48. Kraus, S.; Benard, O.; Naor, Z.; Seger, R. *J. Biol. Chem.* **2003**, *278*, 32618.
49. Naor, Z.; Benard, O.; Seger, R. *Trends Endocrinol. Metab.* **2000**, *11*, 91.
50. Reiss, N.; Llevi, L.; Shacham, S.; Harris, D.; Seger, R.; Naor, Z. *Endocrinology* **1997**, *138*, 1673.
51. Sharman, W.; Van Lier, J.; Allen, C. *Adv. Drug Deliv. Rev.* **2004**, *56*, 53.
52. Grzelak, A.; Rychik, B.; Bartosz, G. *Free Radic. Biol. Med.* **2001**, *30*, 1418.
53. Rosenthal, I. *Photochem. Photobiol.* **1991**, *53*, 859.
54. Szoke, B.; Horvath, J.; Halmos, G.; Rekasi, Z.; Groot, K.; Nagy, A.; Schally, AV. *Peptides* **1994**, *15*, 359.
55. Sobolev, A. S.; Jans, D. A.; Rosenkranz, A. A. *Prog. Biophys. Mol. Biol.* **2000**, *73*, 51.
56. Rahimipour, S.; Ben-Aroya, N.; Ziv, K.; Chen, A.; Fridkin, M.; Koch, Y. *J. Med. Chem.* **2003**, *46*, 3965.
57. Buettner, G. R.; Oberley, L. W. *Biochem. Biophys. Res. Commun.* **1978**, *83*, 69.
58. Atherton, E.; Sheppard, R. C. *Solid Phase Peptide Synthesis—A practical Approach*; IRL Press: Oxford, 1989.
59. Rahimipour, S.; Weiner, L.; Shrestha-Dawadi, P. B.; Bitter, S.; Koch, Y.; Fridkin, M. *Lett. Pept. Sci.* **1998**, *5*, 421.
60. Frisch, M. J.; Trucks, G. W.; Schlegel, H. B.; Scuseria, G. E.; Robb, M. A.; Cheeseman, J. R.; Zakrzewski, V. G.; Montgomery, J. A.; Stratmann, R. E.; Burant, J. C.; Dapprich, S.; Millam, J. M.; Daniels, A. D.; Kudin, K. N.; Strain, M. C.; Farkas, O.; Tomasi, J.; Barone,V.; Cossi, M.; Cammi, R.; Mennucci, B.; Pomelli, C.; Adamo, C.; Clifford, S.; Ochterski, J.; Petersson, G.A.; Ayala, P.Y.; Cui, Q.; Morokuma, K. D.; Malick, K.; Rabuck, A. D.; Raghavachari, K.; Foresman, J. B.; Cioslowski, J.; Ortiz, J. V.; Stefanov, B. B.; Liu, G.; Liashenko, A.; Piskorz, P.; Komaromi, I.; Gomperts, R.; Martin, R. L.; Fox, D.J.; Keith, T.M.; Al-Laham, A.; Peng, C.Y.; Nanayakkara,A.; Gonzalez, C.; Challacombe, M.; Gill, P. M. W.; Johnson, B.; Chen, W.; Wong, M. W.; Andres, J. L.; Gonzalez, C.; Head-Gordon, M. E.; Replogle, S.; Pople, J. A. *Gaussian 98*; Gaussian, Inc.: Pittsburgh, PA, 1998.
61. Daane, T. A.; Parlow, A. F. *Endocrinology* **1971**, *88*, 653.
62. Koch, Y.; Meidan, R.; Chobsieng, P.; Naor, Z. *J. Reprod. Fertil.* **1977**, *50*, 347.